



Article

# Investigating the Molecular Basis of the Aggregation Propensity of the Pathological D76N Mutant of Beta-2 Microglobulin: Role of the Denatured State

Lorenzo Visconti <sup>1,†</sup>, Francesca Malagrino <sup>1,†</sup>, Luca Broggin <sup>2</sup>, Chiara Maria Giulia De Luca <sup>3</sup> , Fabio Moda <sup>3</sup> , Stefano Gianni <sup>1,\*</sup>, Stefano Ricagno <sup>2,\*</sup> and Angelo Toto <sup>1</sup>

<sup>1</sup> Istituto Pasteur-Fondazione Cenci Bolognetti, Dipartimento di Scienze Biochimiche “A. Rossi Fanelli” and Istituto di Biologia e Patologia Molecolari del CNR, Sapienza Università di Roma, 00185 Rome, Italy; lorenzo.visconti@uniroma1.it (L.V.); francesca.malagrino@uniroma1.it (F.M.); Angelo.Toto@uniroma1.it (A.T.)

<sup>2</sup> Dipartimento di Bioscienze, Università degli Studi di Milano, 20133 Milano, Italy; luca.broggin@unimi.it

<sup>3</sup> Fondazione IRCCS Istituto Neurologico Carlo Besta, Divisione di Neurologia 5-Neuropatologia, 20133 Milano, Italy; chiara.deluca@istituto-besta.it (C.M.G.D.L.); Fabio.Moda@istituto-besta.it (F.M.)

\* Correspondence: stefano.gianni@uniroma1.it (S.G.); Stefano.ricagno@unimi.it (S.R.)

† These authors contributed equally to this work.

Received: 27 November 2018; Accepted: 11 January 2019; Published: 18 January 2019



**Abstract:** Beta-2 microglobulin ( $\beta 2m$ ) is a protein responsible for a pathologic condition, known as dialysis-related amyloidosis (DRA), caused by its aggregation and subsequent amyloid formation. A naturally occurring mutation of  $\beta 2m$ , D76N, presents a higher amyloidogenic propensity compared to the wild type counterpart. Since the three-dimensional structure of the protein is essentially unaffected by the mutation, the increased aggregation propensity of D76N has been generally ascribed to its lower thermodynamic stability and increased dynamics. In this study we compare the equilibrium unfolding and the aggregation propensity of wild type  $\beta 2m$  and D76N variant at different experimental conditions. Our data revealed a surprising effect of the D76N mutation in the residual structure of the denatured state, which appears less compact than that of the wild type protein. A careful investigation of the structural malleability of the denatured state of wild type  $\beta 2m$  and D76N pinpoint a clear role of the denatured state in triggering the amyloidogenic propensity of the protein. The experimental results are discussed in the light of the previous work on  $\beta 2m$  and its role in disease.

**Keywords:** protein stability; denatured state; protein aggregation

## 1. Introduction

Several types of human diseases, spanning from Alzheimer’s disease to systemic amyloidosis, are caused by the incorrect folding of proteins [1]. A common factor of such pathological conditions lies in the accumulation of toxic aggregates [2]. Frequently, these aggregates are characterized by a specific type of highly ordered and stable structures, known as amyloid fibers, which are characterized by a conserved cross-beta structure and that can be identified with specific assays [3–5].

Beta-2 microglobulin ( $\beta 2m$ ) is a 99 residue protein forming part of the major histocompatibility complex class I (MHC-I). The aggregation and subsequent amyloid formation of  $\beta 2m$  has been associated with a pathological condition known as dialysis-related amyloidosis (DRA) [6,7]. In fact, in dialyzed patients, there is an abnormally high concentration of  $\beta 2m$  in blood. Such concentration of  $\beta 2m$  exposes DRA patients to the risk of  $\beta 2m$  amyloid deposition, a process that occurs mainly in joints and bones [8]. Intriguingly,  $\beta 2m$  aggregation depends on several molecular properties and

its initiation requires at least partial unfolding of the native state [9,10];  $\beta$ 2m aggregation propensity correlates well with thermodynamic stability [11] but recently an important role for protein dynamics in determining amyloidogenicity was also reported [12,13]. Thus, this protein system represents a suitable candidate to investigate the links between protein folding, misfolding, and pathology.

The first naturally occurring mutant of  $\beta$ 2m was identified in 2012 [14]. This variant is much more aggressively amyloidogenic *in vitro* and *in vivo* compared to wt  $\beta$ 2m and corresponds to a mutation at position 76, where a D is mutated to N. Biophysical characterization of the D76N variant *in vitro* demonstrated that the mutation triggers remarkable effects by decreasing the thermodynamic stability of the protein and increasing its propensity to form amyloids [14,15].

A structural analysis of the D76N mutant compared to the wt  $\beta$ 2m highlighted an interesting conundrum (Figure 1).

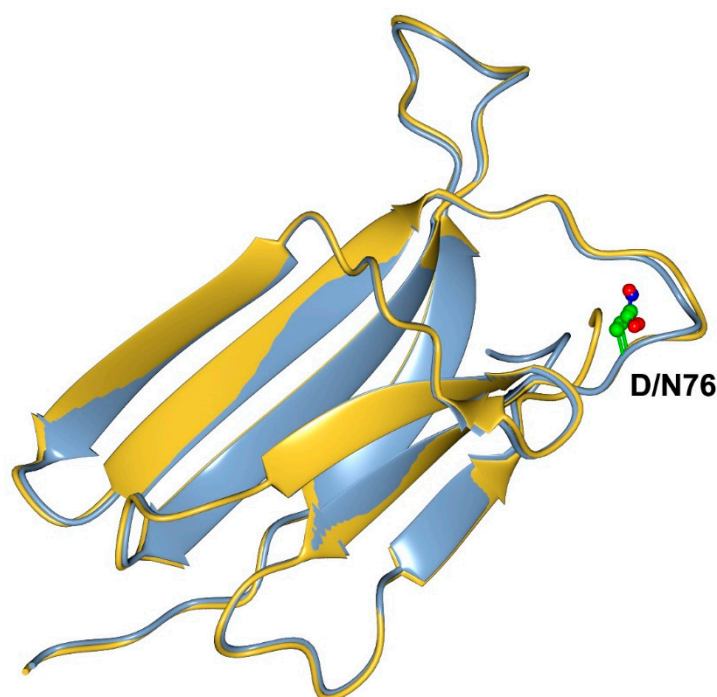


**Figure 1.** Three-dimensional structure of the D76N mutant (blue) in comparison to that of the wild type protein (yellow). Residue 76 is shown in ball and stick representation. It is evident that the native states of the two proteins are perfectly superimposable.

In fact, despite the dramatic effect of the mutation, residue 76 is located on a loop exposed to the solvent and the structure of the mutant is essentially identical to that of the wild type [14]. Thus, a comprehensive analysis of the biophysical and structural data available on D76N demonstrated that the destabilizing effect of the mutation is due to a complex effect involving an increased protein dynamics promoting the accumulation of a high-energy aggregation prone species [16].

Since the effect of the D76N mutation cannot be solely ascribed to direct effects on the native state, here we provide a characterization of the equilibrium folding behavior of the mutant in comparison to that of wt  $\beta$ 2m. Data reveal that the destabilizing effect of the mutation is at least in part due to a change in its denatured state, which appears less compact than that of the wild type protein. Furthermore, by studying the equilibrium denaturation at different experimental conditions, we investigate the links between the compactness of the denatured state and the aggregation propensity of the protein. Our data are briefly discussed in the context of previous work on  $\beta$ 2m.

## 2. Results

### 2.1. Equilibrium Unfolding Experiments

The thermodynamic stabilities of  $\beta 2m$  wt and D76N variant were previously explored using thermal denaturations [16]. These studies showed a destabilization of the mutant, as mirrored by a  $\Delta T_m$  of 10 K. In order to further compare the equilibrium unfolding of  $\beta 2m$  wt and D76N, we conducted GdnHCl-induced equilibrium denaturation experiments. Protein denaturation was monitored by measuring the fluorescence emission of the two tryptophan residues in position 60 and 95 at different concentrations of GdnHCl. In both cases, observed fluorescence was consistent with a simple sigmoidal transition, characteristic of two-state folding. The robustness of the two-state equilibrium transition for both  $\beta 2m$  wt and D76N was further confirmed by fitting globally the fluorescence profiles obtained at different wavelengths with shared thermodynamic parameters. The dependence of the normalized observed fluorescence signal at 330 nm versus the concentration of denaturant for wt and D76N is reported in Figure 2. It is evident that, whilst the mutant unfolds at lower concentrations of GdnHCl, the apparent cooperativity of the transition is affected by the mutation, with an increase of cooperativity for D76N as compared to that of the wild type protein.

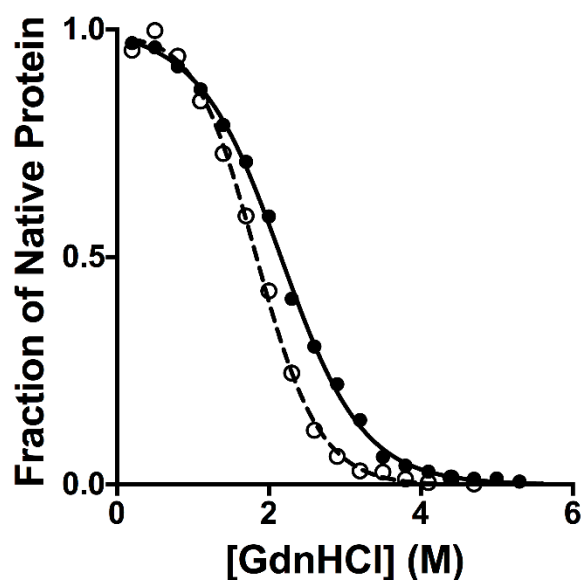


**Figure 2.** Equilibrium denaturations of wild type (full circles) and D76N variant (empty circles) performed in Hepes 50 mM pH 7.0 at 25 °C. The full line (for wild type) and the broken line (for D76N) are the best fit of an equation describing a two state unfolding mechanism. It is evident that the mutant displays a higher cooperativity compared to that of the wild type protein.

A powerful parameter to infer the mechanism of folding single domain proteins is the  $m_{D-N}$  value, defined as  $\partial\Delta G/\partial[\text{denaturant}]$ , which is the quantitative measurement of the cooperativity of the transition. In fact, the  $m_{D-N}$  value is correlated to the change in the accessible surface area to the solvent upon unfolding [17] and allows therefore detecting indirectly the overall structural transition occurring between the native and denatured states. The  $m_{D-N}$  values obtained for  $\beta 2m$  wt and D76N were  $1.08 \pm 0.02 \text{ kcal mol}^{-1} \text{ M}^{-1}$  and  $1.45 \pm 0.04 \text{ kcal mol}^{-1} \text{ M}^{-1}$ , respectively, highlighting an effect of the mutation on the cooperativity of the unfolding reaction. Since it was previously established that  $\beta 2m$  wt and D76N share a nearly identical native state [14], a decreased change in the accessible surface area upon denaturation can be ascribed to a more compact denatured state, highlighting the presence of a residual structure in the denatured state. Thus, on the basis of the comparison between the observed  $m_{D-N}$  values for  $\beta 2m$  wt and D76N it may be concluded that the mutation leads to an expansion of the polypeptide chain in the denatured state.

Since the analysis of  $m_{D-N}$  values represents a signature of the residual structure in denatured states, by challenging the system at different experimental conditions, it is possible to monitor the structural malleability of the denatured state and therefore to characterize its shifts along the reaction coordinate. Thus, we resorted to perform equilibrium unfolding experiments at different experimental conditions, i.e., by varying the pH and ionic strength. The dependence of calculated  $m_{D-N}$  versus pH and the square root of the ionic strength at pH 7.0 for wt and D76N is reported in Figure 3 and the associated folding parameters are listed in Table 1.

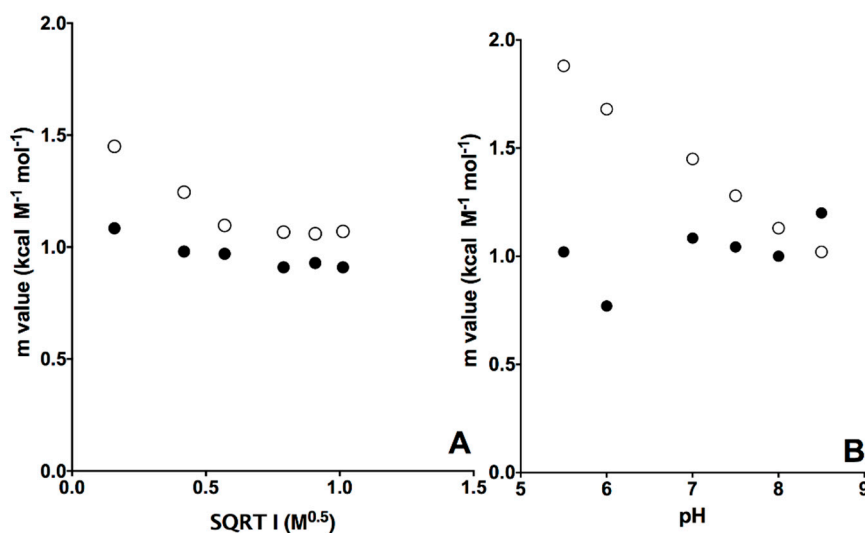


**Figure 3.** Dependence of  $m_{D-N}$  values calculated at different ionic strengths (panel A) and pH (panel B) for wt (full circles) and D76N variant (empty circles).

**Table 1.** Equilibrium folding parameters of wild type and D76N  $\beta 2m$ .

$\beta 2m$ Wild Type			$\beta 2m$ D76N		
$IS^{1/2}$ ( $M^{1/2}$ )	$[GdnHCl]_{1/2}$ (M)	$m_{value}$ ( $\text{kcal M}^{-1} \text{mol}^{-1}$ )	$[GdnHCl]_{1/2}$ (M)	$m_{value}$ ( $\text{kcal M}^{-1} \text{mol}^{-1}$ )	
0.16	$2.12 \pm 0.07$	$1.08 \pm 0.03$	$1.82 \pm 0.02$	$1.45 \pm 0.04$	
0.42	$2.07 \pm 0.09$	$0.98 \pm 0.03$	$2.13 \pm 0.02$	$1.25 \pm 0.03$	
0.57	$2.02 \pm 0.06$	$0.97 \pm 0.05$	$1.95 \pm 0.07$	$1.10 \pm 0.03$	
0.79	$2.12 \pm 0.06$	$1.02 \pm 0.02$	$1.79 \pm 0.03$	$1.07 \pm 0.03$	
0.91	$2.21 \pm 0.06$	$0.93 \pm 0.01$	$2.03 \pm 0.02$	$1.06 \pm 0.04$	
1.01	$1.61 \pm 0.16$	$0.91 \pm 0.06$	$1.42 \pm 0.06$	$1.06 \pm 0.06$	
$\beta 2m$ Wild Type			$\beta 2m$ D76N		
pH	$[GdnHCl]_{1/2}$ (M)	$m_{value}$ ( $\text{kcal M}^{-1} \text{mol}^{-1}$ )	$[GdnHCl]_{1/2}$ (M)	$m_{value}$ ( $\text{kcal M}^{-1} \text{mol}^{-1}$ )	
5.5	<1	$1.02 \pm 0.03$	$1.22 \pm 0.02$	$1.88 \pm 0.04$	
6	$1.40 \pm 0.16$	$0.77 \pm 0.04$	$1.74 \pm 0.02$	$1.74 \pm 0.05$	
7	$2.13 \pm 0.07$	$1.08 \pm 0.03$	$1.81 \pm 0.02$	$1.45 \pm 0.04$	
7.5	$2.09 \pm 0.08$	$1.04 \pm 0.03$	$2.36 \pm 0.02$	$1.28 \pm 0.03$	
8	$2.04 \pm 0.09$	$1.00 \pm 0.03$	$1.77 \pm 0.05$	$1.12 \pm 0.06$	
8.5	$1.95 \pm 0.04$	$1.23 \pm 0.01$	$1.79 \pm 0.03$	$1.02 \pm 0.02$	

Inspection of the experimental data reveals that while the  $m_{D-N}$  value of wild type  $\beta 2m$  is essentially insensitive to pH and ionic strength, for the D76N variant there is an evident decrease of the  $m_{D-N}$  value with increasing pH and ionic strength. Overall, these observations indicate the denatured state of wild type  $\beta 2m$  to be characterized by a malleable residual structure. Such structure is perturbed in D76, but becomes more compact as the pH and ionic strength of the solution increase.

## 2.2. Aggregation Essays

In a recent comprehensive biophysical and structural work, it was proposed that the aggregation properties of D76N to be ascribed to the population of an aggregation-prone, highly dynamic, species, which is more compact and less aggregation prone in the wild type protein [18]. On the light on the equilibrium folding transitions described above, it is tentative to speculate that among these aggregation-prone species the denatured state of the protein may play a role, being more expanded for D76N than that of the wild type protein. A possible test to verify this hypothesis would be represented by the comparison of the aggregation propensity of D76N as a function of ionic strength and pH and the dependence of its associated unfolding  $m_{D-N}$  values.

To this aim, we performed aggregation experiments of D76N (40  $\mu$ M) under continuous shaking at 37 °C under the same conditions of pH and of ionic strength, which are relevant in modifying the compactness of D76N unfolded state. The aggregation kinetics were monitored by thioflavin T showing that the aggregation lag time is increased as pH and ionic strength increase (Figure 4A,B, respectively, where the mean values of the three independent experiments subjected to nonlinear regression analysis, using Boltzmann sigmoidal equation, are reported). ThT fluorescence tends to be more intense in samples, which quickly aggregate suggesting a more abundant amyloid formation under certain conditions; however, fluorescence intensity strongly depends on experimental conditions and should be considered with care.

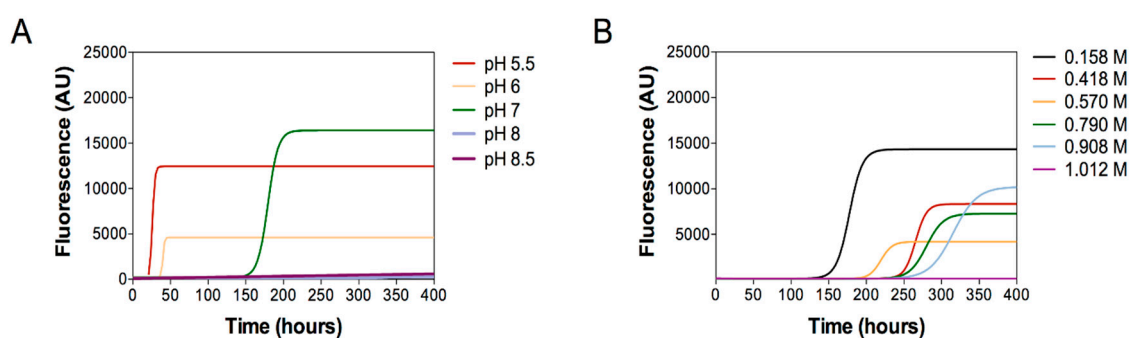


**Figure 4.** Aggregation experiments of D76N as function of pH (panel A) and of ionic strength (panel B). Aggregation was followed by monitoring thioflavin T (ThT) fluorescence. The mean values of the three independent experiments subjected to nonlinear regression analysis, using Boltzmann sigmoidal equation, are reported.

In summary these results clearly showed that D76N aggregation propensity is enhanced by low pH (Figure 4A) and by low ionic strength (Figure 4B). In contrast, high pH conditions or high salt concentrations delay or totally abrogate protein aggregation, even after 400 h of reaction.

## 3. Discussion

The denatured state of proteins has historically received considerably less consideration than the native state. In fact, the latter exerts all the biological functions and characterizing its structure is typically a key step in understanding them. Additionally, addressing denatured states is particularly difficult as they are elusive to the classical structural biology techniques and may be populated only under certain conditions.

In this context, it is important to distinguish between the unfolded state, the highly disordered conformation that may be populated in the presence of denaturant, and the denatured state, which retains a considerable amount of residual structure and represents a transient on-pathway species accumulating only at very low denaturant concentrations (or in the absence of it) [19–21]. Whilst the unfolded state often corresponds to an expanded random coil conformation, the residual structure of the denatured state is critical in sculpting the folding pathways of proteins, as well as in committing the protein to a specific topology [22–27].

The destabilization effects of the pathological D76N mutant of  $\beta 2m$  represents a paradigmatic example on how the structural studies on the sole native state do not provide a full picture on protein stability, being the native state of both variants essentially identical [14,15]. From this angle, the experiments reported in this work are particularly informative as they point out a crucial role to the destabilizing effects in the denatured state induced by the D76N mutation. In fact, the experimental data suggest a scenario whereby the apparent  $\Delta\Delta G$  observed in thermal denaturation experiments is most likely to arise from the expansion, and consequent increase in free energy, of the denatured state rather than changes in the native conformation.

Previous studies on the amyloidogenic properties of  $\beta 2m$  have demonstrated that aggregation might occur only when the protein transiently escapes the thermodynamic well of its native state [9,10]. This finding would suggest that in the case of D76N, there should be a correlation between thermodynamic stability and aggregation propensity. A comparison between the equilibrium unfolding and aggregation data obtained at different pH and ionic strengths, however, shows a much more complex scenario. In fact, while the protein is mildly destabilized at high ionic strengths, it is evident that its thermodynamic stability is essentially insensitive to pH between 8.5 and 7. However, under such conditions D76N displays completely different kinetics of amyloid aggregation. Thus, we conclude that the strong correlation of the amyloidogenic propensity the thermodynamic stability underlies a strong contribution from the overall structure of the denatured state. Increasing amount of data from solid state NMR and Cryo-EM [28–31] show that proteins with an ordered native fold such as  $\beta 2m$  and immunoglobulin light chains display a structural organization in fibrils, which is completely different from the native fold. This observation directly suggests that these proteins need to totally unfold during the aggregation pathway.

The experiments reported in this work indicate that the denatured state has a malleable structure that is perturbed from changes in experimental conditions. The overall compactness of such state correlates with the aggregation propensity of D76N. Overall, our work represents a direct demonstration on the key role of denatured states in dictating protein aggregation and reinforces the importance of their characterization.

## 4. Materials and Methods

### 4.1. Protein Expression and Purification

Recombinant wt and D76N  $\beta 2m$  were expressed and purified as previously reported [12].

### 4.2. Equilibrium Experiments

Equilibrium unfolding experiments on wt and D76N  $\beta 2m$  were performed at 25 °C using a Fluoromax single photon counting spectrofluorometer (Jobin-Yvon; Edison, NJ, USA) and a quartz cuvette with a path length of 1 cm. The native protein, at a constant concentration of 2  $\mu M$ , was mixed with increasing concentrations of the denaturant agent guanidium chloride (GdnHCl), and the intrinsic tryptophan emission of the residues in position 60 and 95 was measured by excitation at 280 nm and record of emission spectra between 300 and 400 nm. Fluorescence equilibrium experiments at different pH were carried out using 50 mM sodium acetate pH 5.5, 50 mM BisTris pH 6.0 pH 6.5, 50 mM HEPES pH 7.0, 50 mM TrisHCl pH 7.5, pH 8.0, and pH 8.5 as buffers. In equilibrium denaturations at different ionic strength conditions, the buffer used was 50 mM HEPES pH 7.0 with different NaCl concentrations (0, 150 mM, 300 mM, 600 mM, 800 mM, and 1000 mM).

Data were fitted using the following equation,

$$Y_{obs} = (Y_N + Y_D) \frac{e^{m_{D-N}([GdnHCl] - [GdnHCl]_{1/2})}}{1 + e^{m_{D-N}([GdnHCl] - [GdnHCl]_{1/2})}}$$

### 4.3. Aggregation Assays

Aggregation assays of D76N  $\beta$ 2m at different pH (5.5, 6, 7, 8, and 8.5) were performed in reaction mix containing D76N  $\beta$ 2m (40  $\mu$ M) and ThT (10  $\mu$ M).

Aggregation assays of D76N  $\beta$ 2m at different concentration of NaCl (0, 150 mM, 300 mM, 600 mM, 800 mM, and 1000 mM) were performed in 25 mM Na phosphate pH 7.4 containing D76N  $\beta$ 2m (40  $\mu$ M) and ThT (10  $\mu$ M).

All reactions were performed in triplicate using black, clear-bottom, 96-well microplates. After sealing, the plate was incubated in a FLUOstar OPTIMA reader (BMG Labtech, Germany) at 37 °C, over a period of 400 h with continuous shaking (600 rpm, single orbital). The ThT fluorescence values are expressed in arbitrary units (AU) and were taken every hour using 450  $\pm$  10 nm (excitation) and 480  $\pm$  10 nm (emission) wavelengths, with a bottom read and a gain of 1000. The mean ThT fluorescence values per sample were plotted against time (hours).

The mean ThT fluorescence values of the three replicates per sample were plotted against time (hours) and the obtained curves were subjected to nonlinear regression analysis, using Boltzmann sigmoidal equation.

**Author Contributions:** S.G., S.R., and A.T. designed the research. L.V., F.M. (Francesca Malagrino), L.B., C.M.G.D.L., F.M. (Fabio Moda) and A.T. performed the research. All the authors analyzed data. S.G. and S.R. wrote the first version of the manuscript. All authors revised the manuscript.

**Acknowledgments:** This work was partly supported by grants from the Italian Ministero dell'Istruzione dell'Università e della Ricerca (Progetto di Interesse 'Invecchiamento' to S.G.), Sapienza University of Rome (C26A155S48, B52F16003410005, and RP11715C34AEAC9B to S.G.), and by grants by Fondazione Cariplo (grant n. 2016-0489) and ARISLA (project TDP-43-STRUCT) to S.R.

**Conflicts of Interest:** The authors declare no conflict of interest.

### References

1. Knowles, T.P.; Vendruscolo, M.; Dobson, C.M. The amyloid state and its association with protein misfolding diseases. *Nat. Rev. Mol. Cell Biol.* **2014**, *15*, 384–396. [[CrossRef](#)] [[PubMed](#)]
2. Westermarck, P.; Benson, M.D.; Buxbaum, J.N.; Cohen, A.S.; Frangione, B.; Ikeda, S.; Masters, C.L.; Merlini, G.; Saraiva, M.J.; Sipe, J.D. A primer of amyloid nomenclature. *Amyloid* **2007**, *14*, 179–183. [[CrossRef](#)] [[PubMed](#)]
3. Chiti, F.; Dobson, C.M. Protein misfolding, functional amyloid, and human disease. *Annu. Rev. Biochem.* **2006**, *75*, 333–366. [[CrossRef](#)] [[PubMed](#)]
4. Chiti, F.; Dobson, C.M. Protein Misfolding, Amyloid Formation, and Human Disease: A Summary of Progress Over the Last Decade. *Annu. Rev. Biochem.* **2017**, *86*, 27–68. [[CrossRef](#)] [[PubMed](#)]
5. Baldwin, A.J.; Knowles, T.P.; Tartaglia, G.G.; Fitzpatrick, A.W.; Devlin, G.L.; Shammass, S.L.; Waudby, C.A.; Mossuto, M.F.; Meehan, S.; Gras, S.L.; et al. Metastability of native proteins and the phenomenon of amyloid formation. *J. Am. Chem. Soc.* **2011**, *133*, 14160–14163. [[CrossRef](#)] [[PubMed](#)]
6. Stoppini, M.; Bellotti, V. Systemic amyloidosis: Lessons from beta2-microglobulin. *J. Biol. Chem.* **2015**, *290*, 9951–9958. [[CrossRef](#)] [[PubMed](#)]
7. Gejyo, F.; Yamada, T.; Odani, S.; Nakagawa, Y.; Arakawa, M.; Kunitomo, T.; Kataoka, H.; Suzuki, M.; Hirasawa, Y.; Shirahama, T.; et al. A new form of amyloid protein associated with chronic hemodialysis was identified as beta 2-microglobulin. *Biochem. Biophys. Res. Commun.* **1985**, *129*, 701–706. [[CrossRef](#)]
8. Gorevic, P.D.; Casey, T.T.; Stone, W.J.; DiRaimondo, C.R.; Prelli, F.C.; Frangione, B. Beta-2 microglobulin is an amyloidogenic protein in man. *J. Clin. Investig.* **1985**, *76*, 2425–2429. [[CrossRef](#)] [[PubMed](#)]
9. McParland, V.J.; Kad, N.M.; Kalverda, A.P.; Brown, A.; Kirwin-Jones, P.; Hunter, M.G.; Sunde, M.; Radford, S.E. Partially unfolded states of beta(2)-microglobulin and amyloid formation in vitro. *Biochemistry* **2000**, *39*, 8735–8746. [[CrossRef](#)] [[PubMed](#)]
10. Smith, D.P.; Jones, S.; Serpell, L.C.; Sunde, M.; Radford, S.E. A systematic investigation into the effect of protein destabilisation on beta 2-microglobulin amyloid formation. *J. Mol. Biol.* **2003**, *330*, 943–954. [[CrossRef](#)]

11. Ami, D.; Ricagno, S.; Bolognesi, M.; Bellotti, V.; Doglia, S.M.; Natalello, A. Structure, stability, and aggregation of beta-2 microglobulin mutants: Insights from a Fourier transform infrared study in solution and in the crystalline state. *Biophys. J.* **2012**, *102*, 1676–1684. [[CrossRef](#)] [[PubMed](#)]
12. Esposito, G.; Ricagno, S.; Corazza, A.; Rennella, E.; Gumral, D.; Mimmi, M.C.; Betto, E.; Pucillo, C.E.; Fogolari, F.; Viglino, P.; et al. The controlling roles of Trp60 and Trp95 in beta2-microglobulin function, folding and amyloid aggregation properties. *J. Mol. Biol.* **2008**, *378*, 887–897. [[CrossRef](#)] [[PubMed](#)]
13. Camilloni, C.; Sala, B.M.; Sormanni, P.; Porcari, R.; Corazza, A.; De Rosa, M.; Zanini, S.; Barbiroli, A.; Esposito, G.; Bolognesi, M.; et al. Rational design of mutations that change the aggregation rate of a protein while maintaining its native structure and stability. *Sci. Rep.* **2016**, *6*, 25559. [[CrossRef](#)] [[PubMed](#)]
14. Valleix, S.; Gillmore, J.D.; Bridoux, F.; Mangione, P.P.; Dogan, A.; Nedelec, B.; Boimard, M.; Touchard, G.; Goujon, J.M.; Lacombe, C.; et al. Hereditary systemic amyloidosis due to Asp76Asn variant beta2-microglobulin. *N. Engl. J. Med.* **2012**, *366*, 2276–2283. [[CrossRef](#)] [[PubMed](#)]
15. Halabelian, L.; Ricagno, S.; Giorgetti, S.; Santambrogio, C.; Barbiroli, A.; Pellegrino, S.; Achour, A.; Grandori, R.; Marchese, L.; Raimondi, S.; et al. Class I major histocompatibility complex, the trojan horse for secretion of amyloidogenic beta2-microglobulin. *J. Biol. Chem.* **2014**, *289*, 3318–3327. [[CrossRef](#)] [[PubMed](#)]
16. De Rosa, M.; Barbiroli, A.; Giorgetti, S.; Mangione, P.P.; Bolognesi, M.; Ricagno, S. Decoding the Structural Bases of D76N ss2-Microglobulin High Amyloidogenicity through Crystallography and Asn-Scan Mutagenesis. *PLoS ONE* **2015**, *10*, e0144061. [[CrossRef](#)] [[PubMed](#)]
17. Myers, J.K.; Pace, C.N.; Scholtz, J.M. Denaturant m values and heat capacity changes: Relation to changes in accessible surface areas of protein unfolding. *Protein Sci.* **1995**, *4*, 2138–2148. [[CrossRef](#)]
18. Le Marchand, T.; de Rosa, M.; Salvi, N.; Sala, B.M.; Andreas, L.B.; Barbet-Massin, E.; Sormanni, P.; Barbiroli, A.; Porcari, R.; Sousa Mota, C.; et al. Conformational dynamics in crystals reveal the molecular bases for D76N beta-2 microglobulin aggregation propensity. *Nat. Commun.* **2018**, *9*, 1658. [[CrossRef](#)]
19. Mittag, T.; Forman-Kay, J.D. Atomic-level characterization of disordered protein ensembles. *Curr. Opin. Struct. Biol.* **2007**, *17*, 3–14. [[CrossRef](#)]
20. McCarney, E.R.; Kohn, J.E.; Plaxco, K.W. Is there or isn't there? The case for (and against) residual structure in chemically denatured proteins. *Crit. Rev. Biochem. Mol. Biol.* **2005**, *40*, 181–189. [[CrossRef](#)]
21. Oliveberg, M.; Fersht, A.R. Thermodynamics of transient conformations in the folding pathway of barnase: Reorganization of the folding intermediate at low pH. *Biochemistry* **1996**, *35*, 2738–2749. [[CrossRef](#)] [[PubMed](#)]
22. Morrone, A.; McCully, M.E.; Bryan, P.N.; Brunori, M.; Daggett, V.; Gianni, S.; Travaglini-Allocatelli, C. The denatured state dictates the topology of two proteins with almost identical sequence but different native structure and function. *J. Biol. Chem.* **2011**, *286*, 3863–3872. [[CrossRef](#)] [[PubMed](#)]
23. Troilo, F.; Bonetti, D.; Toto, A.; Visconti, L.; Brunori, M.; Longhi, S.; Gianni, S. The Folding Pathway of the KIX Domain. *ACS Chem Biol* **2017**, *12*, 1683–1690. [[CrossRef](#)]
24. Giri, R.; Morrone, A.; Travaglini-Allocatelli, C.; Jemth, P.; Brunori, M.; Gianni, S. Folding pathways of proteins with increasing degree of sequence identities but different structure and function. *Proc. Natl. Acad. Sci. USA* **2012**, *109*, 17772–17776. [[CrossRef](#)] [[PubMed](#)]
25. Plaxco, K.W.; Gross, M. Unfolded, yes, but random? Never! *Nat. Struct. Biol.* **2001**, *8*, 659–660. [[CrossRef](#)] [[PubMed](#)]
26. Religa, T.L.; Markson, J.S.; Mayor, U.; Freund, S.M.; Fersht, A.R. Solution structure of a protein denatured state and folding intermediate. *Nature* **2005**, *437*, 1053–1056. [[CrossRef](#)] [[PubMed](#)]
27. Shortle, D.; Ackerman, M.S. Persistence of native-like topology in a denatured protein in 8 M urea. *Science* **2001**, *293*, 487–489. [[CrossRef](#)] [[PubMed](#)]
28. Iadanza, M.G.; Silvers, R.; Boardman, J.; Smith, H.I.; Karamanos, T.K.; Debelouchina, G.T.; Su, Y.; Griffin, R.G.; Ranson, N.A.; Radford, S.E. The structure of a beta2-microglobulin fibril suggests a molecular basis for its amyloid polymorphism. *Nat. Commun.* **2018**, *9*, 4517. [[CrossRef](#)]
29. Barbet-Massin, E.; Ricagno, S.; Lewandowski, J.R.; Giorgetti, S.; Bellotti, V.; Bolognesi, M.; Emsley, L.; Pintacuda, G. Fibrillar vs crystalline full-length beta-2-microglobulin studied by high-resolution solid-state NMR spectroscopy. *J. Am. Chem. Soc.* **2010**, *132*, 5556–5557. [[CrossRef](#)]



30. Liberta, F.; Loerch, S.; Rennegarbe, M.; Schierhorn, A.; Westermark, P.; Westermark, G.T.; Grigorieff, N.; Fandrich, M.; Schmidt, M. Cryo-EM structure of an amyloid fibril from systemic amyloidosis. *bioRxiv* 2018. [[CrossRef](#)]
31. Swec, P.; Lavatelli, F.; Tasaki, M.; Paissoni, C.; Rognoni, P.; Maritan, M.; Brambilla, F.; Milani, P.; Mauri, P.; Camilloni, C.; et al. Cryo-EM structure of cardiac amyloid fibrils from an immunoglobulin light chain (AL) amyloidosis patient. *bioRxiv* 2018. [[CrossRef](#)]



© 2019 by the authors. Licensee MDPI, Basel, Switzerland. This article is an open access article distributed under the terms and conditions of the Creative Commons Attribution (CC BY) license (<http://creativecommons.org/licenses/by/4.0/>).